RSC Advances

This is an *Accepted Manuscript*, which has been through the Royal Society of Chemistry peer review process and has been accepted for publication.

Accepted Manuscripts are published online shortly after acceptance, before technical editing, formatting and proof reading. Using this free service, authors can make their results available to the community, in citable form, before we publish the edited article. This *Accepted Manuscript* will be replaced by the edited, formatted and paginated article as soon as this is available.

You can find more information about *Accepted Manuscripts* in the **Information for Authors**.

RSC Advances

PAPER

A series of codendrimers from polyamidoamine (PAMAM) and oligoethylene glycols (OEG) dendrons as drug carriers: The effects of OEG dendron decorated degree

Yanna Zhao,[a] Jing Zhao,[b] Ran Li,[a] Meihua Han,[a] Chunyan Zhu,[a] Mincan Wang,[b] Yifei Guo,*[a] and Xiangtao Wang*[a]

A series of codendrimers (co-D$_{64}$, co-D$_{48}$, co-D$_{32}$, and co-D$_{16}$) from polyamidoamine (PAMAM) decorated by oligoethylene glycols (OEG) dendron with similar structure but different decorated degree (DD) were prepared, their properties in aqueous solution, including particle size and morphology, were investigated. To explore interactions between codenderimers and drug, then find the effects of OEG dendron decorated degree, these codendrimers were utilized as drug carrier to load methotrexate (MTX). Although these drug-loaded nanoparticles presented the similar particle size, morphology, thermal transition, and physical state, it was proved that codendrimers with lower DD (co-D$_{32}$, 50%; co-D$_{16}$, 25%) were the most suitable carrier to load MTX from the results of drug-loading content (DLC), entrapment efficiency (EE), and cytotoxicity, due to the stronger hydrophobic and electrostatic interaction between the free amine group of codendrimers and MTX. The results from drug release profiles indicated release kinetics was not only controlled by these interactions, the steric hindrance of OEG dendron should be considered. Overall, co-D$_{32}$ with moderate decorated degree could be a promising drug delivery system.

1. Introduction

Design and creation of novel nanoscale drug delivery system (NDDS) to transport anticancer drug to tumor tissue is one of the challenging and rapidly growing fields of research. PAMAM dendrimers with extremely precise and controlled architecture are a unique class of synthetic polymers and play an important role in NDDS.[1-3] PAMAM dendrimer-based drug carriers can enhance the solubility, improve bioavailability, and reduce the harmful side effects of these drugs, furthermore the narrow molecular weight distributions can provide reproducible pharmacokinetic behaviour.[4]

Drug molecules can be transferred either by covalently bonded on the PAMAM dendrimer surface or physical entrapped into the dendrimer core.[5, 6] For physical entrapment, the hydrophobic drugs could be encapsulated by dendrimres via hydrogen bonds,[7] electrostatic interactions between oppositely charged fragments of drug molecule and dendrimer macromolecule,[8, 9] and hydrophobic interactions.[8] As one of the most effective delivery system, PAMAM dendrimers with primary amine groups (PAMAM-NH$_2$) are utilized as drug carrier broadly to achieve the relative high drug-loading content (DLC) and stability, owing to the electrostatic interaction and hydrogen bonding interaction between amine groups and drugs.[9-13] Besides, PAMAM-NH$_2$ could promote cellular uptake due to the tight junctions between positively charged amine groups and oppositely charged cellular membrane.[14-16]

[a.] Institute of Medicinal Plant Development, Chinese Academy of Medical Sciences & Peking Union Medical College, Beijing 100193, P. R. China.E-mail: ffguo@163.com, xtaowang@163.com; Fax: +86-10-57833266; Tel: +86-10-57833266
[b.] The College of Chemistry and Molecular Engineering, Zhengzhou University, Zhengzhou, Henan Province 450052, P. R. China

However, PAMAM-NH$_2$ dendrimers present high cytotoxicity *in vivo*,[17, 18] and result in eliminated rapidly from circulation and accumulated in the liver, kidney, lung, and spleen.[19-22] Notably, various modifications of primary amine groups covering PAMAM's surface have been explored to develop PAMAM-based derivatives or alter dendrimer terminal charges in order to reduce cytotoxicity, control clearance and biodistribution in the body.[23-26] For this purpose, dendrimers are generally modified with PEG chains,[27, 28] acylation,[29, 30] targeting molecules,[31, 32] peptides,[33, 34] carbohydrates,[35] amino acids,[36, 37] or drugs.[38, 39] Since the decoration reagents react with amine groups on PAMAM periphery, the modified degree is designed as high as possible to reduce the cytotoxicity maximum, which may cause insufficient charge reduction and/or may reduce DLC.[40]

In our previous study, the oligoethylene glycol (OEG) dendrons were utilized to modify the PAMAM G4.0, the codendrimer PAMAM-co-OEG (co-D$_{64}$) with the 100% decorated degree was synthesized, and the drug-loading capacity of this novel codendrimer was explored.[41] Furthermore, to find the suitable hydrophobic drugs and explain the encapsulation mechanism, various drugs were tested and methotrexate (MTX) was found to be the most suitable drug entrapped by co-D$_{64}$, likely due to the stronger electrostatic interactions between amino groups of codendrimers and carboxyl groups of MTX.[42] Considering this kind of codendrimer could include different structural subtype depending on the decorated degree of OEG dendron and co-D$_{64}$ is only one of them, it was easily supposed that less OEG dendron may lead to better MTX-loading efficacy due to the enhanced electrostatic interactions. Besides, the surface positive charge of codendrimers with less OEG dendron could be helpful to cellular uptake and promote DLC.[27] It is necessary to prepare a series codendrimers from PAMAM and OEG dendron with different

decorated degree (DD), and further research the interactions between these codendrimers and MTX.

In the present study, a series of codendrimers **co-D$_{64}$, co-D$_{48}$, co-D$_{32}$,** and **co-D$_{16}$** with 100%, 75%, 50%, and 25% DD were prepared
5 separately (Fig. 1), and MTX was selected as the model drug to evaluate these codendrimers as drug carrier. The effect of OEG dendron on the DLC, stability of MTX-loaded nanoparticles, *in vitro* release profiles, cytotoxicity against MCF-7 cells were investigated, furthermore, their physicochemical properties were researched.
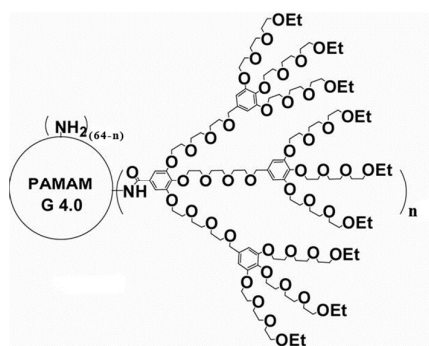
10

Fig. 1 Structure of the series of codendrimers (**co-D$_{64}$**, n = 64; **co-D$_{48}$**, n = 48; **co-D$_{32}$**, n = 32; **co-D$_{16}$**, n = 16)

2. Experimental section

15 **2.1 Materials**

The codendrimers (**co-D$_{48}$, co-D$_{32}$**) were synthesized according to pervious papers.[41] Methotrexate (MTX, purity >98%) was purchased from Shanghai Heng Yuan Bio-Tech Co., Ltd. (Shanghai, China). Other reagents and solvents were purchased at reagent
20 grade and used without further purification. Silica gel 300-400 mesh was used as the stationary phase for column chromatography. All samples were dried thoroughly under vacuum prior to analytical measurements to remove solvent molecules.

The human breast cancer cell line (MCF-7) was purchased from
25 the Institute of Basic Medical Science, Chinese Academy of Medical Science (Beijing, China). RPMI-1640 was purchased from Hyclone Thermo Scientific (America). Fetal bovine serum (FBS, 10%) was purchased from Gibco Thermo Scientific (America), and 100 unit mL^{-1} penicicillin G and streptomycin were purchased from
30 Biotopped Science & Technology Co., Ltd. (Beijing, China).

2.2 Syntheses

2.2.1 Synthesis of codendrimer co-D$_{48}$

The solution of OEG dendron active ester (1.42 g, 0.55 mmol) in DMF (20 mL) was added into a solution of PAMAM G4.0 (150 mg,
35 10.5 μmol), TEA (102 mg, 1.01 mmol), and DMAP (20 mg) in a mixed solvent DMF/H$_2$O (40 mL, 1/1, v/v) at -5 °C with stirring, and the reaction temperature was allowed to raise to room temperature. After stirring for 36 h, the solvents were evaporated *in vacuo* at room temperature, the residue was purified by column
40 chromatography with DCM as eluent, afforded codendrimer **co-D$_{48}$**

as a colorless oil (1.23 g, 82%). ^{1}H NMR (600 MHz, DMSO-d$_6$): δ = 1.05 (br, CH$_3$), 2.21 (br, CH$_2$), 2.43 (br, CH$_2$), 2.66 (br, CH$_2$), 3.37 (br, CH$_2$), 3.41 (br, CH$_2$), 3.47 (br, CH$_2$), 3.49-3.60 (br, CH$_2$), 3.63 (br, CH$_2$), 3.69 (br, CH$_2$), 3.96 (br, CH$_2$), 4.03 (br, CH$_2$), 4.08 (br, CH$_2$),
45 4.38 (br, CH$_2$), 6.57 (br, CH), 7.17 (br, CH), 7.80 (br, NH), 8.02 (br, NH), 8.45 (br, NH); ^{13}C NMR (DMSO-d$_6$): δ = 14.58, 38.76, 39.24, 39.38, 39.68, 39.70, 45.46, 66.24, 68.06, 68.54, 69.68, 69.70, 69.74, 69.94, 74.47, 76.22, 105.00, 138.68, 139.44, 156.94 ppm. Elemental analysis (%) calcd for C$_{6286}$H$_{10944}$N$_{250}$O$_{2476}$, 129576.68: C, 58.21%; H,
50 8.53%; N, 2.70%. Found: C, 58.02%; H, 8.06%; N, 2.21%.

2.2.2 Synthesis of codendrimer co-D$_{32}$

The solution of OEG dendron active ester (1.27 g, 0.49 mmol) in DMF (10 mL) was added into a solution of PAMAM G4.0 (200 mg, 15.3 μmol), TEA (68 mg, 0.67 mmol), and DMAP (20 mg) in mixed
55 solvent DMF/H$_2$O (30 mL, 1/1, v/v) at -5 °C with stirring, and the reaction temperature was allowed to raise to room temperature. After stirring for 24 h, the solvents were evaporated *in vacuo* at room temperature, the residue was purified by column chromatography with DCM as eluent, afforded codendrimer **co-D$_{32}$**
60 as a colorless oil (1.01 g, 86%). ^{1}H NMR (600 MHz, DMSO-d$_6$): δ = 1.06 (br, CH$_3$), 2.21 (br, CH$_2$), 2.43 (br, CH$_2$), 2.50 (br, CH$_2$), 2.73 (br, CH$_2$), 3.09 (br, CH$_2$), 3.19 (br, CH$_2$), 3.27 (br, CH$_2$), 3.38-3.97 (br, CH$_2$), 4.04 (br, CH$_2$), 4.10 (br, CH$_2$), 4.35 (br, CH$_2$), 6.58 (br, CH), 7.86 (br, NH), 8.08 (br, NH), 8.49 (br, NH); ^{13}C NMR (DMSO-d$_6$): δ =
65 12.68, 36.08, 38.12, 39.02, 39.72, 39.98, 46.06, 68.24, 68.69, 68.90, 69.45, 69.79, 69.84, 69.91, 75.87, 76.92, 106.06, 135.65, 138.41, 158.09 ppm. Elemental analysis (%) calcd for C$_{3776}$H$_{7712}$N$_{250}$O$_{1692}$, 91120.27: C, 57.92%; H, 8.55%; N, 3.84%. Found: C, 57.19%; H, 8.52%; N, 3.61%.

70 **2.3 Characterization of codendrimers-NMR and GPC**

^{1}H NMR spectra were recorded on a Bruker AV 600 (600 MHz) spectrometer, and chemical shifts were reported as δ values (ppm) relative to internal Me$_4$Si. Gel permeation chromatography (GPC) measurements were carried out on a Viscotek GPC VE2001
75 instrument with single column set equipped with refractive index detector and DMF (containing 1 g L^{-1} LiBr) as the eluent at 35 °C. Calibration was performed with PMMA standards.

2.4 Preparation of drug-loaded nanoparticles

Drug-loaded nanoparticles were prepared by the dialysis method.
80 Briefly, the codendrimers (8 mg) and methotrexate (MTX, 4 mg) were dissolved in DMF (1 mL) in the glass vials at room temperature, and then the deionized water (5 mL) was added dropwise into these vials at 4 °C under vigorous stirring. The mixed solution was transferred into the dialysis bag (MWCO 14000) and
85 dialyzed against deionized water (4 × 1 L) for 4 h to remove DMF and free MTX. To quantify the entrapment efficiency (EE) and drug-loading content (DLC), the drug in the nanoparticles was collected by lyophilized and analyzed by HPLC (UltiMate3000, DIONEX) using a UV detector operated at 306 nm. The quantitative analysis was
90 carried out on a Thermo C18 (4.60 mm × 250 mm, 5 μm) and compared to a calibration curve generated from 9:1 PBS (0.01 M):CH$_3$CN (y = 1.36x + 0.03, R^2 = 0.9999). The flow rate was 0.8 mL min^{-1}, and the sample injection volume was 20 μL. The EE and DLC were calculated as follows, the experiments were conducted in

triplicates, and the data were shown as the mean values plus standard deviation (± SD).

EE = (weight of loaded drug/weight in feed) × 100%
DLC = (weight of loaded drug/weight of drug-loaded codendrimer) × 100%

2.5 Hydrodynamic size and zeta potential measurements

The hydrodynamic size and zeta potential were determined by dynamic light scattering (DLS) using a Zetasizer Nano-ZS analyzer (Malvern Instruments, UK) with an integrated 4 mV He-Ne laser, λ = 633 nm, which used the backscattering detection (scattering angle θ = 173°) at room temperature. Samples were prepared in deionized water at a concentration of 2 mg mL^{-1}. The experiments were conducted in triplicates. The data were shown as the mean values plus standard deviation (± SD).

2.6 Transmission electron microscope

Transmission electron microscope (TEM) studies were performed with a JEM-1400 instrument (JEOL, Japan) at an accelerating voltage of 80 kV. Samples were prepared by drop-casting codendrimer solutions onto carbon-coated copper grids, air-drying them at room temperature and then dyeing with uranyl acetate solution (2%, w/v).

2.7 Differential scanning calorimetry

Differential scanning calorimetry (DSC) measurements were carried out with a DSC Q200 (TA Co., USA) using aluminum pans with lids, MTX mixed with codendrimers in the same ratio of MTX-loaded nanoparticles were used for all the experiments, under dynamic nitrogen atmosphere. Thermograms were obtained by heating the samples from 20 to 280 °C with a scan rate of 10 °C min^{-1}.

2.8 X-ray diffraction analysis

The X-ray diffraction analysis (XRD) was performed for the pure MTX, physical mixture of MTX and codendrimers, and MTX-loaded nanoparticles, using a Japan D/Max 2500PC X-ray diffractomer (Rigaku, Japan) with a 2θ range between 3° and 80° using graphite filtered Cu-K$_\alpha$ radiation (λ = 1.54 Å) at 40 KV and 100 mA (scanning rate of 8° min^{-1}). The XRD patterns were recorded under ambient temperature conditions.

2.9 *In vitro* drug release

The MTX-loaded nanoparticle solutions (0.5 mL) were transferred into a dialysis bags (MWCO 14000). They were immersed in 50 mL of 150 mM NaCl solution. The release studies were performed at 37 °C with continuous magnetic stirring at 100 rpm. At predetermined time intervals, 5 mL of the external solution was withdrawn for analysis and an equal volume of fresh media was replenished. The drug release study was performed for 48 h. The amount of MTX released was analyzed with a UV-HPLC. The release experiments were conducted in triplicates. The data were shown as the mean values plus standard deviation (± SD).

2.10 MTT assay

The cytotoxicity against human breast cancer cell line (MCF-7 cells) was assessed by an MTT assay. Briefly, cells were cultured in RPMI-1640 medium supplemented with 10% fetal calf serum, and 100 units mL^{-1} penicicillin G and streptomycin at 37 °C with 5% CO$_2$ and seeded in 96-well plates at a density of 8000 cells per well. After incubation for 24 h, the growth medium was replaced with fresh RPMI-1640. Then, the codendrimer solutions, MTX-loaded nanoparticles, and control (free MTX) were added into the wells. After incubation for 48 h, 10 µL MTT solutions were added to each well and incubation were continued for another 4 h. The medium was removed and 200 µL DMSO was added into each well to dissolve the formazan by pipetting up and down for several times. The absorbance of solution in each well was measured using an ELISA plate reader at a test wavelength of 570 nm to determine the OD value. The cell inhibition rate was calculated as follows. Cell inhibition = (1-OD$_{treated}$/OD$_{control}$) × 100%, where OD$_{treated}$ was obtained for the cells treated by the nanoparticles, OD$_{control}$ was obtained for the cells treated by the culture medium, and the other culture conditions were the same. Each experiment was done in quintuplicates. The data were shown as the mean values plus standard deviation (± SD).

2.11 Statistical analysis

The results obtained from hydrodynamic diameter, drug-loading and release experiments, cytotoxicity were expressed as the mean ± standard deviation (SD). Statistical analysis was performed with SPSS 19.0 software. Student's t-test was used to evaluate the differences between groups, and P<0.05 was considered significant.

Scheme 1 Synthetic procedure for codendrimers[a]
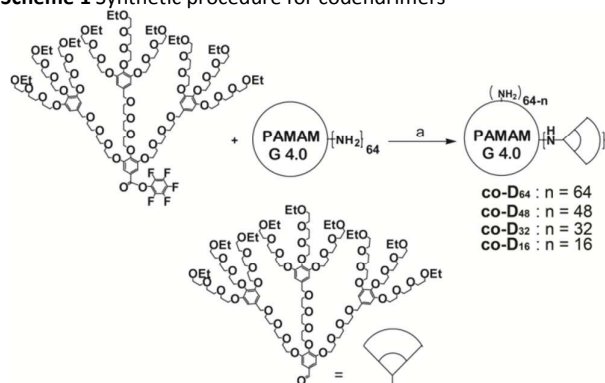
[a] Reagent and conditions: (a) TEA, DMAP, DMF, -5-25 °C, 24 h (87%, 82%, 86%, and 85% for **co-D$_{64}$**, **co-D$_{48}$**, **co-D$_{32}$**, and **co-D$_{16}$**). TEA = triethylamine, DMAP = N, N-dimethylaminopyridine, DMF = dimethylformamide.

3. Results and discussion

3.1 Synthesis and characterization of codendrimers

The series of codendrimers were synthesized according to previous reports,[41] and the synthesis procedures are shown in Scheme 1. The peripheral primary amine groups of fourth-generation PAMAM were decorated by OEG dendron through "attach-to" route to prepare codendrimers with different decorated degree (DD), including **co-D$_{64}$** (100% DD), **co-D$_{48}$** (75% DD), **co-D$_{32}$** (50% DD), and

ARTICLE

co-D$_{16}$ (25% DD). After purification by column chromatography with DCM as eluent, all the yields were above 80% (Table 1).

All these codendrimers were characterized by ^{1}H NMR spectroscopy in DMSO-d$_6$ (Fig. 2). The peaks at 1.10 ppm corresponded to methyl units in the OEG dendrons (marked by b) and signals at 2.22 ppm (marked by a) were attributed to methylene units in the PAMAM. With increasing DD from 25% to 100%, the signals intensity of PAMAM core decreased relative to the signals of the OEG dendritic shell which was likely due to the shielding effect of OEG dendron.[43] The molar masses of these four codendrimers were determined by GPC with DMF as the eluent, and the result are shown in Table 1. With increasing the DD, the molar masses increased significantly and the polydispersity decreased. Comparing with the original material PAMAM only dissolved in water, the series codendrimers were all highly soluble in DCM, THF, MeOH, DMF, and H$_2$O, on account of the excellent solubility of the outer OEG dendritic shell.

Table 1 Synthetic conditions and results for codendrimers

Entries	DD^a (%)	Time (h)	Yield (%)	GPC results^b		D$_h$^{c} (nm)	ζ^d (mV)
				Mn ×10^{-5}	PDI		
co-D$_{64}$	100	48	87	1.89	1.00	82.6 ± 19.2	25.8 ± 2.9
co-D$_{48}$	75	36	82	1.37	1.01	75.5 ± 16.5	27.7 ± 1.0
co-D$_{32}$	50	24	86	0.94	1.03	87.3 ± 12.8	41.4 ± 2.0
co-D$_{16}$	25	24	85	0.46	1.03	93.4 ± 14.1	43.1 ± 0.6

^{a} Decorated degree. ^{b} All GPC measurements were performed with DMF (1 g L^{-1} LiBr) as eluent at 35 °C. ^{c} D$_h$: hydrodynamic diameter, 2 mg mL^{-1}, DLS detected, n = 3. ^{d} ζ: zeta potential, 2 mg mL^{-1}, DLS detected, n = 3.
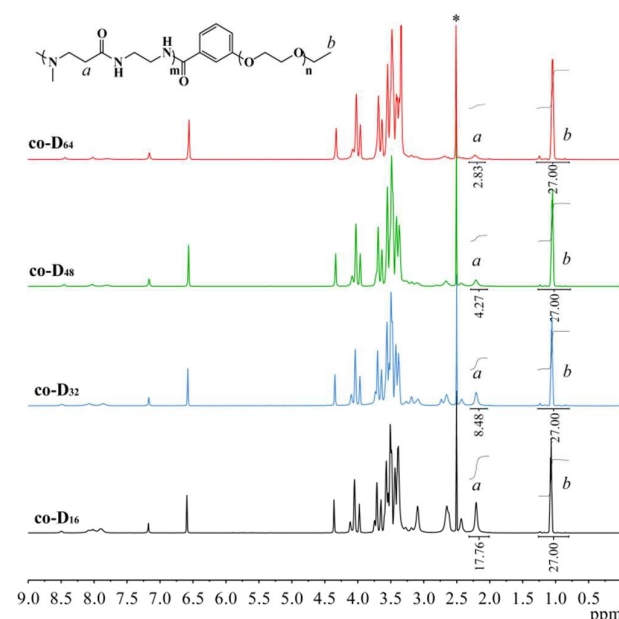

Fig. 2 ^{1}H NMR spectra of codendrimers. The intensity of PAMAM G4.0 signals decreases systematically with increasing decorated degree which is especially clear for the signal at approximately δ = 2.22 ppm.

The particle size and zeta potential in aqueous solution of the series codendrimers were measured by dynamic light scattering (DLS). These four codendrimers showed the similar mean hydrodynamic diameter (approximately 90 nm, Table 1), but the different particle size distribution curves (Fig. 3). For codendrimers **co-D$_{64}$** and **co-D$_{48}$** with higher DD, they demonstrated a bimodal distribution with a smaller-sized component of approximately 8 nm and a large-sized component of approximately 230 nm, indicating the two type particles (unimers and aggregates) existed in these two solutions. While, for codendrimers **co-D$_{32}$** and **co-D$_{16}$** with lower DD, size of about 100 nm was observed which presented a high aggregation. The PAMAM core of **co-D$_{32}$** and **co-D$_{16}$** could not be covered completely by OEG dendritic shell due to the low DD, similar as other amphiphilic polymers; they formed aggregates in aqueous solution. With increasing the DD, the PAMAM core could be covered gradually, the stability of codendrimer was enhanced, therefore, these codendrimers could exist as unimers in aqueous solution, and two peaks were found in the particle size distribution curves.
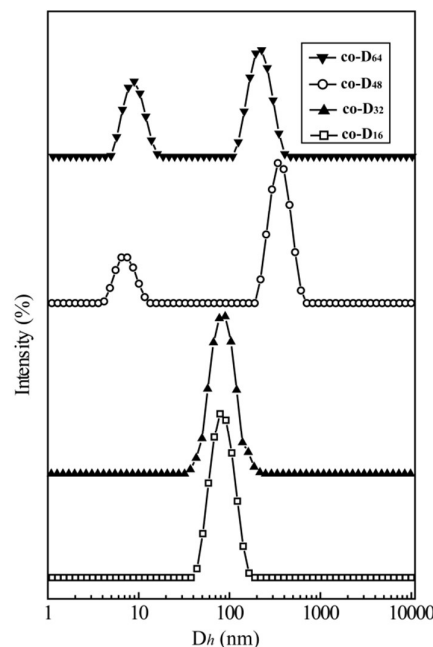

Fig. 3 DLS graph of the size distribution of codendrimers in aqueous solutions at room temperature with concentration of 2 mg mL^{-1}.

This phenomenon was also reflected in TEM observation (Fig. 4). These micrographs revealed that the series of codendrimers presented different aggregation behavior, both unimers (marked with arrows) and aggregates were observed massively presented in

aqueous solution for **co-D$_{64}$** and **co-D$_{48}$** (Fig. 4a and 4b),[41] while only aggregates were observed for **co-D$_{32}$** and **co-D$_{16}$** (Fig. 4c and 4d).
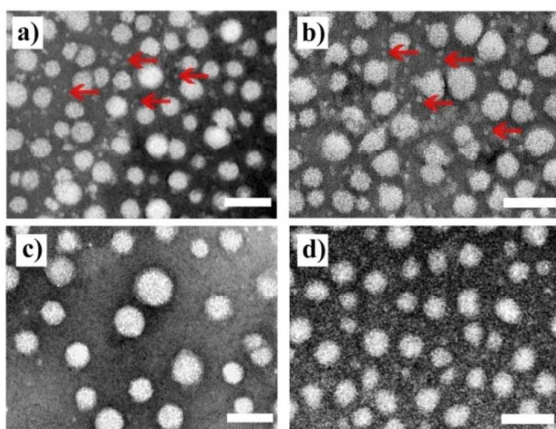
Fig. 4 TEM images of codendrimers **co-D$_{64}$** (a), **co-D$_{48}$** (b), **co-D$_{32}$** (c), and **co-D$_{16}$** (d). Scale bar: 100 nm.

In contrast to the hydrodynamic diameter, different conjugation ratio of OEG dendron to native PAMAM dendrimer caused a significant change in zeta potential. Increasing the DD from 25% to 100% resulted in decrease in zeta potential values from 43.1 to 25.8 mV (Table 1), it seemed that OEG dendritic shell had a shielding effect over primary amines,[34] which was consistent with the result of ^{1}H NMR.

Table 2 Properties of MTX-loaded nanoparticles

Entries	EE^a (%)	DLC^a (%)	D_h^{b} (nm)	ζ^{b} (mV)
D$_{64}$-MTX^c	46.6 ± 3.2	18.9 ± 1.0	98.0 ± 7.2	3.2 ± 0.7
D$_{48}$-MTX^d	51.1 ± 3.1	20.4 ± 1.0	110.7 ± 0.6	4.3 ± 0.4
D$_{32}$-MTX^e	79.6 ± 1.0	28.5 ± 0.4	117.2 ± 4.7	18.4 ± 0.8
D$_{16}$-MTX^f	85.4 ± 0.3	29.9 ± 0.1	117.1 ± 1.0	19.6 ± 0.1

^{a} UV-HPLC detected, n = 3. ^{b} DLS detected, n = 3. ^{c} **D$_{64}$-MTX**: MTX-loaded **co-D$_{64}$** nanoparticles. ^{d} **D$_{48}$-MTX**: MTX-loaded **co-D$_{48}$** nanoparticles. ^{e} **D$_{32}$-MTX**: MTX-loaded **co-D$_{32}$** nanoparticles. ^{c} **D$_{16}$-MTX**: MTX-loaded **co-D$_{16}$** nanoparticles.

3.2 Preparing drug-loaded nanoparticles

To evaluate these codendrimers as the drug carriers and further explore the interactions between codendrimers and drug, several hydrophobic drugs, including MTX, hexamethylmelamine (HMM), and resveratrol (RES) were selected as the model drug to prepare the drug-loaded nanoparticles. MTX could be encapsulated into all of these codendrimers successfully; however, different EE and DLC were obtained. Increasing the DD from 25% to 100%, the EE was decreased from 85.4% to 46.6%, and the DLC was changed from 29.9% to 18.9% respectively (Table 2). On the contrary, it was apparent that the DLC showed no significant difference (p > 0.05) between each drug-loaded nanoparticles for HMM (~5%) and RES (~15%) separately, suggesting the DLC was not affected by the decorated degree of OEG dendron (supporting information, Table S1). This could be explained by the interactions between hydrophobic drug and carriers, including hydrophobic interaction

and electrostatic interactions.[42] The absence of carboxyl group in the structure of HMM and RES presented no electrostatic interactions between drugs and codendrimers, which induced low DLC and no significant difference between each groups. Although the series MTX-loaded nanoparticles could perform the similar hydrophobic interaction due to same PAMAM core and anticancer drug, the different electrostatic interaction between the residual primary amine groups of PAMAM in theses codendrimers and MTX might induce the different DLC value.[44-46] These results suggested that **co-D$_{32}$** and **co-D$_{16}$** would be the suitable carriers for MTX.

3.3 Stability of MTX-loaded nanoparticles

The stability of nanoparticles can be measured by estimating the surface charges using the zeta potential, higher surface charge or higher value of zeta potential means that the nanoparticles are electrostatically repulsive, and thus more stable in solution.[47, 48] The result of zeta potential was in good agreement with EE values, higher DD (**co-D$_{64}$**, **co-D$_{48}$**) resulted in lower zeta potential value (approximately 4 mV, Table 2), and lower DD (**co-D$_{32}$**, **co-D$_{16}$**) resulted in higher zeta potential value (approximately 19 mV, Table 2). These results suggested that **D$_{32}$-MTX** and **D$_{16}$-MTX** nanoparticles could be more stable in aqueous solution, and supported **co-D$_{32}$** and **co-D$_{16}$** would be the suitable carriers.
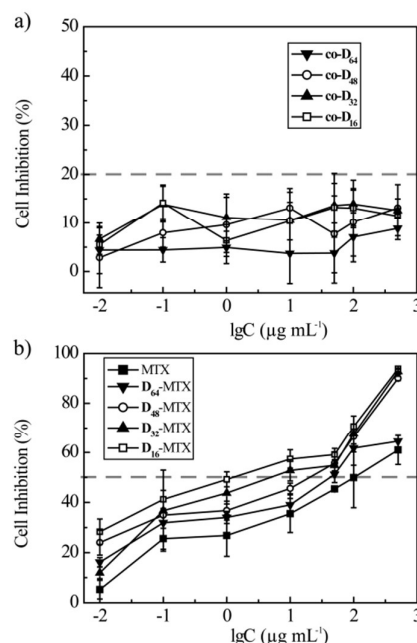

Fig. 5 Cytotoxicity of codendrimers (a) and MTX-loaded nanoparticles (b) against MCF-7 cells for 48 h incubation.

3.4 MTT assay

The cytotoxicity of MTX-loaded codendrimers against MCF-7 cells was determined by MTT assay (Fig. 5). After incubation for 48 h, no significant adverse effect (cell inhibition < 20%) against MCF-7 cells up to a tested concentration of 0.5 mg mL^{-1} was demonstrated in these codendrimers (Fig. 5a), indicating the biocompatible feature of these drug carriers. To compare the cytotoxicity of MTX-loaded nanoparticles, free MTX was used as control. The 50% cellular growth inhibition (IC$_{50}$) was determined as 59.5, 13.9, 11.0, 4.4 and

2.7 µg mL^{-1} for free MTX, **D$_{64}$-MTX**, **D$_{48}$-MTX**, **D$_{32}$-MTX**, and **D$_{16}$-MTX** respectively. The cell inhibition rate of these nanoparticles against MCF-7 cells enhanced significantly (P<0.01) when compared with the free MTX at an equivalent MTX concentration 5 (Fig. 5b), which was most probably because of the suitable size for easy endosome. Besides, it was also found that **D$_{32}$-MTX**, **D$_{16}$-MTX** showed the higher cytotoxicity during these MTX-loaded nanoparticles. There was no significant difference (P>0.05) was obtained between **D$_{32}$-MTX**, and **D$_{16}$-MTX**, declaring the feasibility 10 of **co-D$_{32}$** and **co-D$_{16}$** to be applied as drug carrier.
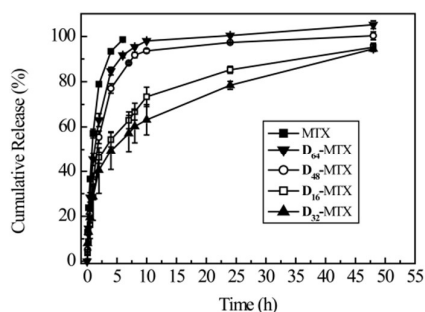

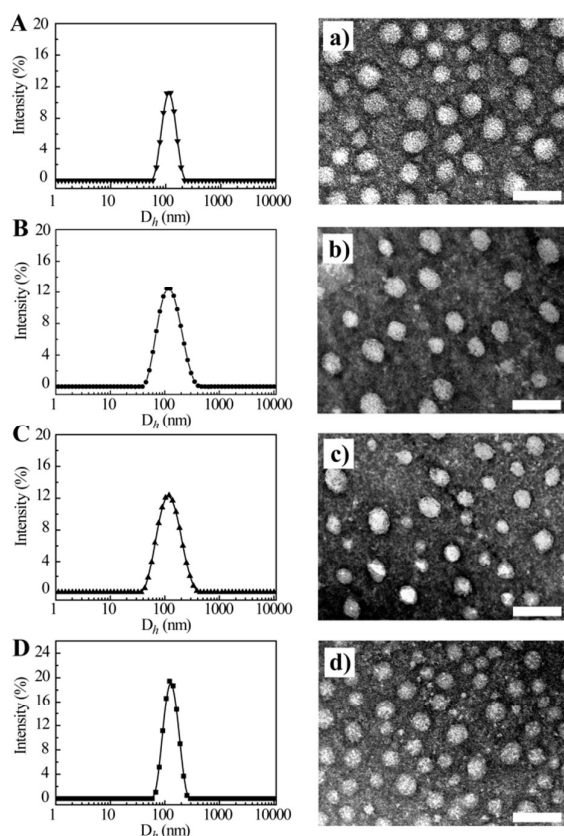**Fig. 6** Cumulative MTX release in 150 mM NaCl solution at 37 °C within 48 h.

15 **Fig. 7** Size distribution curves and TEM images of MTX-loaded nanoparticles: **D$_{64}$-MTX** (A, a), **D$_{48}$-MTX** (B, b), **D$_{32}$-MTX** (C, c), **D$_{16}$-MTX** (D, d). Scale bar: 100 nm.

3.5 *In vitro* release behavior

To further verify the capacity of these codendrimers as drug 20 carrier, the *in vitro* release profiles of MTX-loaded nanoparticles were evaluated in 150 mM NaCl solution at 37 °C. A control experiment using free MTX was also carried out under similar conditions, and the results are shown in Fig. 6. For free MTX, complete diffusion across the dialysis membrane was found to 25 occur within 4 h. MTX-loaded nanoparticles presented the biphasic release procedure, with initial burst release followed by a slow release. All these MTX-loaded nanoparticles were sustained release for 48 h, but the release rate were different significantly. For **D$_{64}$-MTX** and **D$_{48}$-MTX**, above 80% MTX was released from 30 nanoparticles within the initial 5 h, but for **D$_{32}$-MTX** and **D$_{16}$-MTX**, approximately 50% MTX was released. These two codendrimers with higher DD presented higher release rate was likely due to the relative lower interaction between codendrimers and MTX. **D$_{32}$-MTX** performed the slower release rate comparing with **D$_{16}$-MTX**, 35 illustrating the release procedure was not only controlled by interaction between carrier and drug, the contribution of the OEG dendron should be considered. The outer OEG dendritic shell of codendrimers was less flexible and stiffer with increasing the DD from 25% to 50%, hence, the MTX release procedure was 40 hampered by steric hindrance of OEG dendron. The result of release *in vitro* demonstrated that **co-D$_{32}$** was the better carrier.

3.6 Particle size and morphology of MTX-loaded nanoparticles

As these codendrimers could be used as drugs carrier, the feature of MTX-loaded nanoparticles was detected further. All of these 45 nanoparticles showed the mean hydrodynamic diameters of approximately 110 nm (Table 2). Drug loading of codendrimers had slightly effect on their particle sizes, the particle size was increased from 90 to 110 nm, illustrating incorporation of MTX within the nanoparticles generally enlarges their size.[49] Besides, the 50 morphology of these nanoparticles were investigated by TEM observation, all of these nanoparticles were dispersed as individual particles with the regularly spherical shape, and the mean diameter was approximately 40 nm (Fig. 7). The variation in particle size measured by TEM and particle-size analyzer was attributed to the 55 fact that dynamic light scattering (DLS) measurement of the particle size analyzer gave the hydrodynamic diameter rather than the actual diameter of the dried particles. The appropriate particle size (< 200 nm) of MTX-loaded nanoparticles benefited to avoid reticuloendothelial system uptake and achieve passive tumor 60 targeting through EPR effect. From these results, it was clear that the particle sizes and morphology of drug-loaded nanoparticles could not be affected by DD.

3.7 DSC and XRD analysis

To confirm the existing state of MTX in drug-loaded nanoparticles, 65 differential scanning calorimetry (DSC) was utilized to elucidate the thermal transitions of MTX in bulk, in a physical mixture and within drug-loaded nanoparticles analyses (Fig. 8) The thermogram of MTX showed a sharp endothermic peak at 148 °C, which was associated with the melting of MTX.[50] The curve of blank 70 codendrimer **co-D$_{32}$** exhibited no endotherm during the whole heating procedure. The melting endothermic peak of MTX also appeared in the physical mixture of MTX and **co-D$_{32}$**, but disappeared in **D$_{32}$-MTX**. Other drug-loaded nanoparticles showed

the similar thermograms as **D$_{32}$-MTX** (not shown). These results verified the state of MTX in drug-loaded nanoparticles was not physical mixed simply, the interactions between MTX and codendrimers caused these changes.
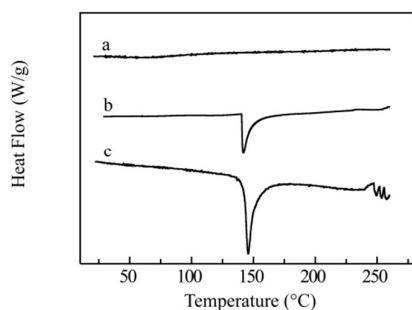

Fig. 8 DSC thermograms of **D$_{32}$-MTX** nanoparticles (a), the physical mixture of MTX and **co-D$_{32}$** (b), and free MTX (c).
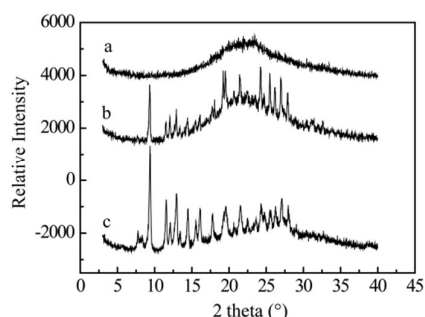

Fig. 9 XRD of **D$_{32}$-MTX** nanoparticles (a), the physical mixture of MTX and **co-D$_{32}$** (b), and free MTX (c).

X-ray powder diffraction was also used to confirm the state of MTX in drug-loaded nanoparticles. Free MTX bulk powder, physical mixture, and **D$_{32}$-MTX** nanoparticles were measured, the results are shown in Fig. 9. The intense peaks indicative MTX existed as the crystalline compound, which could be observed from the spectra of MTX bulk powder and physical mixture of MTX and **co-D$_{32}$**. While, in the **D$_{32}$-MTX** nanoparticles, the characteristic diffraction peaks of MTX powder disappeared, illustrating MTX existed as a molecular dispersion due to the interaction between MTX and **co-D$_{32}$**, which was in good agreement with the result from DSC. Other drug-loaded nanoparticles showed the similar curves as **D$_{32}$-MTX** (not shown).

The results from DSC and XRD suggested the state of MTX in these nanoparticles was not related with the structure of these codendrimers.

Conclusions

Based on the successful synthesis, the series codendrimers (**co-D$_{64}$**, **co-D$_{48}$**, **co-D$_{32}$**, and **co-D$_{16}$**) from PAMAM G4.0 decorated by OEG dendron with different decorated degree were prepared, their structure was confirmed by ^{1}H NMR spectra. In contrast with the particle sizes and morphology, the zeta potential of these codendrimers was dependent on the OEG dendron decorated degree (DD) due to the shielding effects. After loaded anticancer

drug methotrexate (MTX), the mean diameter of the nanoparticles was enlarged from 90 to 110 nm. The DSC and XRD measurements indicated that MTX existed as a molecular dispersion in the drug-loaded nanoparticles and there was no free drug on the surface of nanoparticles. Due to the stronger electrostatic interactions between **co-D$_{32}$**, **co-D$_{16}$** (lower DD) and MTX, **D$_{32}$-MTX** and **D$_{16}$-MTX** showed the higher EE values (approximately 80%) and better stability in aqueous solution. Comparing with free MTX, the cytotoxicity of MTX-loaded nanoparticles against MCF-7 cells was significantly enhanced. *In vitro* release demonstrated that MTX could be sustained release from MTX-loaded nanoparticles in 150 mM NaCl solution for 48 h, and **D$_{32}$-MTX** showed the slower release rate because of the steric hindrance of outer OEG dendritic shell. In conclusion, as the drug carrier, the DD of OEG dendron in codendrimers affected the drug-loading content due to the hydrophobic interactions and electrostatic interactions. While, the drug release profiles were not only controlled by these interactions, the contribution of the OEG dendron should be considered. These results suggested that **co-D$_{32}$** with moderate decorated degree could be a promising drug delivery system.
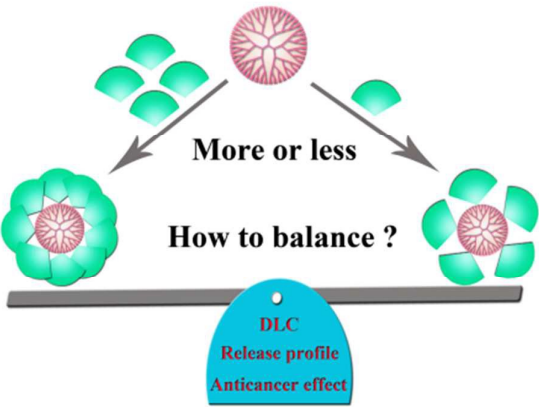
Acknowledgements

Notes and references

1 J. M. Oliveira, A. J. Salgado, N. Sousa, J. F. Mano and R. L. Reis, *Prog. Polym. Sci.,* 2010, **35**, 1163-1194.

2 P. Kesharwani, K. Jain and N. K. Jain, *Chem. Commun.,* 2014, **39**, 268-307.

3 X. Wang, Y. He, J. Wu, C. Gao and Y. Xu, *Biomacromolecules,* 2010, **11**, 245-251.

4 D. A. Tomalia, *Prog. Polym. Sci.,* 2005, **30**, 294-324.

5 S. Svenson, *Eur. J. Pharm. Biopharm.,* 2009, **71**, 445-462.

6 L. M. Kaminskas, V. M. McLeod, C. J. H. Porter and B. J. Boyd, *Mol. Pharm.,* 2012, **9**, 355-373.

7 U. Gupta, H. B. Agashe, A. Asthana and N. K. Jain, *Biomacromolecules,* 2006, **7**, 649-658.

8 A. D'Emanuele and D. Attwood, *Adv. Drug Deliver. Rev.,* 2005, **57**, 2147-2162.

9 E. Markatou, V. Gionis, G. D. Chryssikos, S. Hatziantoniou, A. Georgopoulos and C. Demetzos, *Int. J. Pharm.,* 2007, **339**, 231-236.

10 A. Buczkowski and B. Palecz, *J. Chem. Thermodyn.,* 2014, **70**, 95-100.

11 A. Buczkowski, S. Sekowski, A. Grala, D. Palecz, K. Milowska, P. Urbaniak, T. Gabryelak, H. Piekarski and B. Palecz, *Int. J. Pharm.,* 2011, **408**, 266-270.

12 J. Cao, H. Zhang, Y. Wang, J. Yang and F. Jiang, *Spectrochimica Acta Part A: Molecular and Biomolecular Spectroscopy,* 2013, **108**, 251-255.

13 B. Klajnert and M. Bryszewska, *Bioelectrochemistry,* 2007, **70**, 50-52.

14 M. El-Sayed, M. Ginski, C. Rhodes and H. Ghandehari, *J. Control. Release,* 2002, **81**, 355-365.

15 F. P. Seib, A. T. Jones and R. Duncan, *J. Control. Release,* 2007, **117**, 291-300.

16 S. Wang, Y. Li, J. Fan, Z. Wang, X. Zeng, Y. Sun, P. Song and D. Ju, *Biomaterials,* 2014, **35**, 7588-7597.

17 S. Sadekar and H. Ghandehari, *Adv. Drug Deliver. Rev.,* 2012, **64**, 571-588.

18 E. Frohlich, *Int. J. Nanomedicine,* 2012, **7**, 5577-5591.

19 S. Nigavekar, L. Sung, M. Llanes, A. El-Jawahri, T. Lawrence, C. Becker, L. Balogh and M. Khan, *Pharmaceut. Res.,* 2004, **21**, 476-483.

20 N. Malik, R. Wiwattanapatapee, R. Klopsch, K. Lorenz, H. Frey, J. W. Weener, E. W. Meijer, W. Paulus and R. Duncan, *J. Control. Release,* 2000, **65**, 133-148.

21 A.-N. Petit, T. Debenest, P. Eullaffroy and F. Gagné, *Nanotoxicology,* 2012, **6**, 315-326.

22 T. P. Thomas, I. Majoros, A. Kotlyar, D. Mullen, M. M. Banaszak Holl and J. R. Baker, *Biomacromolecules,* 2009, **10**, 3207-3214.

23 R. B. Kolhatkar, K. M. Kitchens, P. W. Swaan and H. Ghandehari, *Bioconjugate Chem.,* 2007, **18**, 2054-2060.

24 J. B. Wolinsky and M. W. Grinstaff, *Adv. Drug Deliver. Rev.,* 2008, **60**, 1037-1055.

25 R. Jevprasesphant, J. Penny, R. Jalal, D. Attwood, N. B. McKeown and A. D'Emanuele, *Int. J. Pharm.,* 2003, **252**, 263-266.

26 G. Thiagarajan, K. Greish and H. Ghandehari, *Eur. J. Pharm. Biopharm.,* 2013, **84**, 330-334.

27 S. Zhu, M. Hong, G. Tang, L. Qian, J. Lin, Y. Jiang and Y. Pei, *Biomaterials,* 2010, **31**, 1360-1371.

28 H. He, Y. Li, X.-R. Jia, J. Du, X. Ying, W.-L. Lu, J.-N. Lou and Y. Wei, *Biomaterials,* 2011, **32**, 478-487.

29 S. H. Medina and M. E. H. El-Sayed, *Chem. Rev.,* 2009, **109**, 3141-3157.

30 L. Albertazzi, M. Serresi, A. Albanese and F. Beltram, *Mol. Pharm.,* 2010, **7**, 680-688.

31 H. Zong, T. P. Thomas, K.-H. Lee, A. M. Desai, M.-h. Li, A. Kotlyar, Y. Zhang, P. R. Leroueil, J. J. Gam, M. M. Banaszak Holl and J. R. Baker, *Biomacromolecules,* 2012, **13**, 982-991.

32 L. Wang, Z. Wang, G. Ma, W. Lin and S. Chen, *Langmuir,* 2013, **29**, 8914-8921.

33 L. Han, R. Huang, S. Liu, S. Huang and C. Jiang, *Mol. Pharm.,* 2010, **7**, 2156-2165.

34 J. L. Santos, D. Pandita, J. Rodrigues, A. P. Pêgo, P. L. Granja, G. Balian and H. Tomás, *Mol. Pharm.,* 2010, **7**, 763-774.

35 M. K. Calabretta, A. Kumar, A. M. McDermott and C. Cai, *Biomacromolecules,* 2007, **8**, 1807-1811.

36 W. Shi, S. Dolai, S. Rizk, A. Hussain, H. Tariq, S. Averick, W. L'Amoreaux, A. El Idrissi, P. Banerjee and K. Raja, *Org. Lett.,* 2007, **9**, 5461-5464.

37 E. N. Cline, M.-H. Li, S. K. Choi, J. F. Herbstman, N. Kaul, E. Meyhöfer, G. Skiniotis, J. R. Baker, R. G. Larson and N. G. Walter, *Biomacromolecules,* 2013, **14**, 654-664.

38 R. S. Navath, A. R. Menjoge, B. Wang, R. Romero, S. Kannan and R. M. Kannan, *Biomacromolecules,* 2010, **11**, 1544-1563.

39 S. K. Choi, A. Myc, J. E. Silpe, M. Sumit, P. T. Wong, K. McCarthy, A. M. Desai, T. P. Thomas, A. Kotlyar, M. M. B. Holl, B. G. Orr and J. R. Baker, *ACS Nano,* 2013, **7**, 214-228.

40 T. Uehara, D. Ishii, T. Uemura, H. Suzuki, T. Kanei, K. Takagi, M. Takama, M. Murakami, H. Akizawa and Y. Arano, *Bioconjugate Chem.,* 2010, **21**, 175-181.

41 Y. Guo, Y. Zhao, M. Han, C. Hao and X. Wang, *J. Mater. Chem. B,* 2013, **1**, 6078-6084.

42 Y. Guo, Y. Zhao, J. Zhao, M. Han, A. Zhang and X. Wang, *Bioconjugate Chem.,* 2014, **25**, 24-31.

43 Y. Guo, J. D. van Beek, B. Zhang, M. Colussi, P. Walde, A. Zhang, M. Kröger, A. Halperin and A. Dieter Schlüter, *J. Am. Chem. Soc.,* 2009, **131**, 11841-11854.

44 L. J. Twyman, A. E. Beezer, R. Esfand, M. J. Hardy and J. C. Mitchell, *Tetrahedron Letters,* 1999, **40**, 1743-1746.

45 P. Kolhe, E. Misra, R. M. Kannan, S. Kannan and M. Lieh-Lai, *International Journal of Pharmaceutics,* 2003, **259**, 143-160.

46 C. Kojima, K. Kono, K. Maruyama and T. Takagishi, *Bioconjugate Chemistry,* 2000, **11**, 910-917.

47 S. Ghosh, A. H. Khan and S. Acharya, *J. Phys. Chem. C,* 2012, **116**, 6022-6030.

48 C. Wilhelm, C. Billotey, J. Roger, J. N. Pons, J. C. Bacri and F. Gazeau, *Biomaterials,* 2003, **24**, 1001-1011.

49 B. Hoang, R. M. Reilly and C. Allen, *Biomacromolecules,* 2012, **13**, 455-465.

50 N. Vadia and S. Rajput, *European Journal of Pharmaceutical Sciences,* 2012, **45**, 8-18.

Graphical Abstract

Color graphic	
Text	To evaluate the effect of OEG dendron decorated degree and find out the suitable carrier, a series of codendrimers are prepared and utilized to transport methotrexate.